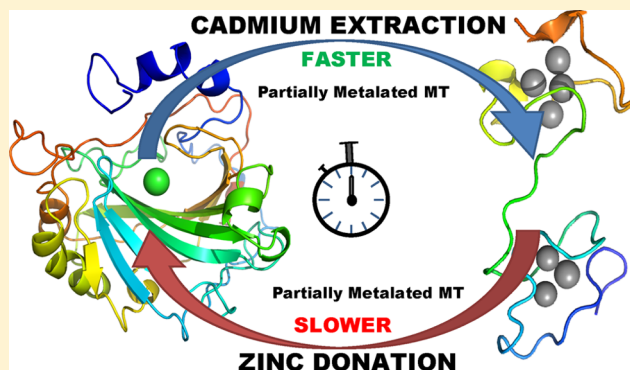


Kinetics of Zinc and Cadmium Exchanges between Metallothionein and Carbonic Anhydrase

Tyler B. J. Pinter and Martin J. Stillman*

Department of Chemistry, The University of Western Ontario, London, Ontario Canada, N6A 5B7

ABSTRACT: The flexible coordination stoichiometry of a relatively high number of metal ions is a property unique to the metallothionein (MT) family of proteins. Mammalian MTs, for example, accommodate up to seven divalent metal ions in tetrahedral coordination geometries, using its complement of 20 cysteine ligands. The lability of the metals from these metaloclusters has been used to support the proposal of MTs acting as metal chaperones, by donating to other metal-binding proteins. The metal exchange kinetics between human MT1A and carbonic anhydrase (CA) were examined using time-dependent electrospray ionization mass spectrometry (ESI-MS). The time dependence of three different reaction conditions were studied: (i) zinc donation from partially metalated zinc-MT to apoCA; (ii) metal exchange between zinc saturated MTs and cadmium saturated CA (Cd-CA); and (iii) metal exchange between partially metalated zinc-MTs and Cd-CA. The results show that zinc donation from Zn-MTs to apo-zinc-dependent enzymes is dependent on the metal loading of the Zn_n -MT (where $n = 1-7$) and that this is a direct consequence of the increasing metal affinity for smaller values of n . Partially metalated MTs are also shown to extract cadmium from Cd-CA with significantly faster rates than metal saturated MTs and that even under zinc limiting conditions, mammalian Cd-CA would not coexist with MT. On the basis of these and previously published results, we suggest that protein–protein interactions between MT and CA facilitate metal transfers through favorable electrostatic interactions and hypothesize that the metal could be transferred between the MT and the enzyme active site using nearby metal-binding functionalities along the transfer pathway.



Mammalian metallothioneins (MT) are small, multiple-metal binding proteins with roles in zinc homeostasis, cadmium detoxification, and cellular redox chemistry.^{1–4} Using the 20 thiols of the cysteine residues, MTs bind up to seven divalent metals into two peptide-wrapped metal–thiolate clusters.⁵ This rather unusual, highly flexible metal coordination system permits metal binding with variable coordination geometries and stoichiometries. Metals bound can be readily donated in exchange reactions depending on the relative metal binding affinities. For example, MTs have a higher affinity for cadmium than for zinc. This allows for exchange with and release of zinc from Zn-MTs concomitant with cadmium binding and sequestration.^{6,7}

Cadmium enters cells adventitiously via essential metal ion transport channels where it associates with proteins containing metal-binding residues.⁸ These associations may disrupt the protein structure or displace legitimate metals, rendering the protein nonfunctional. MTs scavenge cadmium with an exceptionally high average binding affinity [$\log_{10}(K_F) > 10^{14}$] and sequester the toxic cadmium into relatively inert binding sites, potentially protecting the cell against possible toxicological effects.⁹ Cellular cadmium exposure also upregulates MT gene synthesis, creating new apoMT and restoring metal homeostasis.^{10–15}

Relatively few details of the mechanisms involved in these metal exchange processes are currently available. Scavenging by apoMT for cadmium weakly associated with metal binding functionalities on the surfaces of proteins (and other cellular macromolecules) occurs rapidly.¹⁶ The scavenging ability of Zn-MTs is slightly slower due to the occupied binding sites; however, the high binding affinity difference between zinc and cadmium results in exchange reactions for free cadmium added to Zn-MTs *in vitro*.¹⁷

A more important situation arises when cadmium is bound into a zinc binding site of a metalloenzyme having, normally, a catalytically active zinc in the active site. These active sites are usually not solvent exposed and are often buried within the protein fold, a requirement for the activity and specificity of the reaction being catalyzed.¹⁸ Thus, these metal sites are much less accessible and are sterically hindered toward ligand exchange of the bound metal. This means that removal of a toxic metal, such as a cadmium bound to a zinc binding site, would be more difficult. Therefore, the reactions between cadmium substituted zinc-dependent enzymes and Zn-MTs are expected to be

Received: August 17, 2015

Revised: September 23, 2015

Published: September 24, 2015

slower and would likely require involvement of protein–protein interactions (PPIs).

Cadmium bound to a cadmium-specific algal CA (CDCA) has been isolated under zinc limiting conditions, though there are significant differences in the metal binding sites between the cadmium specific algal CA and mammalian Zn-CA.^{19–21} This paper explores the metal exchange properties for a mammalian cadmium-containing CA to provide more details on the metal exchange mechanisms that may occur between MT and a zinc-dependent enzyme. We have investigated the kinetics of metal exchanges between MT and Cd- and Zn-carbonic anhydrase (CA). Three experimental situations have been studied kinetically using electrospray ionization mass spectrometry (ESI-MS): (i) determination of the kinetics of zinc donation from Zn_{4–7}-MT to apoCA under MT limiting conditions, to mimic zinc metalation of a metalloenzyme under zinc-limiting conditions; (ii) determination of the kinetics of metal exchange between zinc saturated MTs, with no open binding sites and Cd-CA, to determine the reaction with fully metalated MT and Cd-CA; and (iii) determination of the kinetics of metal exchange in the presence of open binding sites on Zn_n-MT (where $n = 3–6$) and Cd-CA, to mimic the situation with low cellular zinc and cadmium containing carbonic anhydrase. The results from these experiments suggest that even under zinc-depleted mammalian cellular conditions Cd-CA would not coexist with MT.

METHODS

Purification of Recombinant MT1A. Recombinant human MT1A was purified following previously published procedures.²² The DNA sequence corresponding to our human MT1A amino acid sequence, which contains additional tetra-alanine repeats at the termini and domain-linker region compared to WT human MT1A: MGKAAAACSC ATGGS-CTCTG SCKCKECKCN SCKKAAAACC SCCPMSCAKC AQGCVCKGAS EKSCCKKAA AA was inserted as an N-terminal S-tag fusion into a pET29a plasmids and transformed into BL21(DE3) competent *Escherichia coli* cells and stored as glycerol stocks at -80°C .

Briefly, cells were cultured into 4 L batches of cadmium-spiked LB (Miller) broth, MT expression was induced when $\text{OD}_{600} \approx 0.5$, and cells were harvested following ~ 4 h induction period. MT was purified as the cadmium-saturated form using SP anion exchange columns (GE Lifesciences). The S-tag was removed with thrombin CleanCleave kits (Sigma) and separated from the MT using the SP cartridges. The protein was concentrated and stored in aliquots at -80°C .

Preparation of Zinc Metallothionein. All solutions were vacuum degassed and argon saturated to impede cysteine oxidation. Reducing agents were not added as these affect the kinetics of metal exchange. Samples of Cd-MT were thawed under a vacuum and acidified to pH 2.5 with formic acid. The released cadmium was separated from the apoprotein using Sephadex G-25 (fine) size exclusion media (GE Lifesciences) equilibrated and eluted with argon saturated, formic acid in water, pH 2.8. Protein elution was followed using a Cary 50 equipped with a flow-cell cuvette monitoring the 200–300 nm range. The apoMT was concentrated and buffer exchanged to 5 mM ammonium formate, pH 7.4 buffer under argon using 3K MWCO Amicon Ultra-4 (Millipore) filter units. A small fraction of the concentrated apoMT was remetalated with cadmium and the concentration determined using $\epsilon_{250\text{ nm}} = 89\,000\text{ M}^{-1}\text{ cm}^{-1}$.

Excess zinc acetate was added to the apoMT and allowed to react for 30 min. The excess zinc was separated from the Zn₇-MT by centrifugation in 3K MWCO filters, exchanged with 5 mM ammonium formate, pH 7.4 under argon. The final concentration of the Zn₇-MT was determined spectrometrically by adding excess cadmium to a small fraction of the Zn₇-MT, as described above (cadmium displaces zinc stoichiometrically). The complete replacement of cadmium for zinc and zinc saturation for the Zn-MT was confirmed by ESI-MS.

Preparation of Apocarbonic Anhydrase and Cadmium–Carbonic Anhydrase. Ten milligrams of bovine erythrocyte Zn-CA (Sigma) was dissolved in 4 mL of 5 mM ammonium formate, pH 5.5 buffer containing 50 mM pyridine-2,6-dicarboxylic acid zinc chelator (PDC). This was loaded into a prewashed 10K MWCO Amicon Ultra-4 centrifugal filter unit and concentrated to 500 μL . Approximately 4 mL of fresh PDC containing buffer was added to the concentrated protein and again centrifuged. This process was repeated until all of the zinc was removed from the CA and no zinc was detected in the filtrate. In general, approximately 25 mL (six additions of fresh PDC) were required to remove all of the zinc. The PDC was then removed from the protein by adding 5 mM ammonium formate, pH 7.4 buffer to the filter unit and spinning out the low molecular weight PDC. This process was repeated until no PDC was detected in the filtrate. In total, approximately 50 mL of PDC-free buffer was required to remove all of the PDC from the protein.

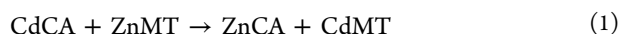
Cd-CA was made by adding 3 \times excess cadmium acetate to the apoCA stock and incubating for 1 h at room temperature. The excess cadmium was removed by centrifugation in 10K MWCO filter exchanged with 5 mM ammonium formate, pH 7.4. The Cd-CA concentrations were determined by UV spectroscopy using $\epsilon_{280\text{ nm}} = 54\,000\text{ M}^{-1}\text{ cm}^{-1}$.^{23,24} The metal content of the Cd-CA was verified by ESI-MS prior to experiments and generally showed greater than 95% replacement of zinc for cadmium.

Reactions between Zn-MT and apoCA or Cd-CA and ESI-MS Parametrization. Zn-MT was added to apoCA or Cd-CA in 5 mM ammonium formate, pH 7.0 buffer under argon and loaded into a gastight syringe (Hamilton), and the reaction was followed by ESI-MS. The solution was infused at 10 $\mu\text{L}/\text{min}$ for continuous data collection using a modified, temperature-controlled syringe pump thermostated to the desired temperature ($\pm 0.5^{\circ}\text{C}$). ESI mass spectral data were collected on a Bruker Micro-TOF II (Bruker Daltonics) operated in the positive ion mode calibrated with NaI as an external calibrant. The settings used were scan = 500–4000 m/z ; rolling average = 2; nebulizer = 2 bar; dry gas = 80°C @ 8.0 L/min; capillary = 4000 V; end plate offset = -500 V ; capillary exit = 175 V; Skimmer 1 = 30.0 V; Skimmer 2 = 23.5 V; Hexapole RF = 800 V.

Data Treatment and Kinetic Analyses. ESI mass spectra were averaged for a minimum of 2 min to ensure good signal-to-noise ratios and deconvoluted using the Maximum Entropy algorithm of the Compass DataAnalysis software package (Bruker Daltonics). Relative peak intensities were extracted from these deconvoluted spectra and plotted as a function of reaction times. These data were fit to lines using Origin 7 SR2 (OriginLab, Northampton, MA) as guides.

The kinetic data were fit to pseudo-second order reaction mechanisms, assuming that all zinc came from the Zn-MT species and all cadmium from the Cd-CA and also that [Cd-

CA] = [Zn-MT] at $t = 0$. Under these assumptions, the second order rate law for Cd-CA reacting with Zn-MT



,is

$$\begin{aligned} \text{rate} &= -\frac{d[\text{CdCA}]}{dt} = -\frac{d[\text{ZnMT}]}{dt} = \frac{d[\text{ZnCA}]}{dt} \\ &= \frac{d[\text{CdCA}]}{dt} \end{aligned} \quad (2)$$

,or

$$-\frac{d[\text{CdCA}]}{dt} = k[\text{ZnMT}][\text{CdCA}] \quad (3)$$

and from the competition experiment we know that

$$[\text{ZnMT}] = [\text{CdCA}] \quad (4)$$

then

$$\frac{d[\text{CdCA}]}{dt} = -k[\text{CdCA}]^2 \quad (5)$$

rearranging gives

$$\frac{d[\text{CdCA}]}{[\text{CdCA}]^2} = -k \, dt \quad (6)$$

integrated is

$$\frac{1}{[\text{CdCA}]_t} = kt + \frac{1}{[\text{CdCA}]_0} \quad (7)$$

Thus, a plot of $1/[\text{CdCA}]_t$ vs t is linear with slope = k and intercept = $1/[\text{CdCA}]_0$. Equation 7 was plotted for each of the three reactions and used to determine the apparent second order rate constants. When the concentrations of Zn-MT and Cd-CA are not equal, a different form of the second-order rate constant must be used. When the concentrations are close, then the subsequent fitting errors are small.

RESULTS

The results for three experiments, each designed to investigate possible cellular zinc and cadmium competition chemistries between MT and CA, are described in the sections below. These experiments probe the effects of metal loading on zinc donation and/or cadmium exchange between MT and CA. The first experiment is limiting in Zn-MT relative to apoCA and tests the effect of low zinc on the donation of zinc to apoCA; the second experiment used Zn₇-MT and Cd-CA in equal concentrations to test the exchange of cadmium for zinc in Zn₇-MT; and the third experiment shows the results for metal exchange between partially metalated Zn-MT and Cd-CA to test the effect of limiting zinc on the exchange of cadmium for zinc in CA. Together, these three experimental data sets provide an understanding of the distribution of cadmium when both MT and CA coexist in the presence of zinc.

Kinetics of the Reaction between Zn₇-MT and apoCA under MT-Limiting Conditions. We devised an experiment where excess apoCA could compete with Zn-MT for its bound zinc in order to evaluate the zinc donation properties of partially metalated Zn-MTs [Zn_{*n*}-MT ($n < 7$)]. The zinc exchange between Zn-MT and apoCA in a 0.75:1.0 ratio (protein/protein) was followed continuously via ESI-MS. Figure 1 shows the time course for the metalation of apoCA by Zn-MT. The charge states of the mass spectral data are

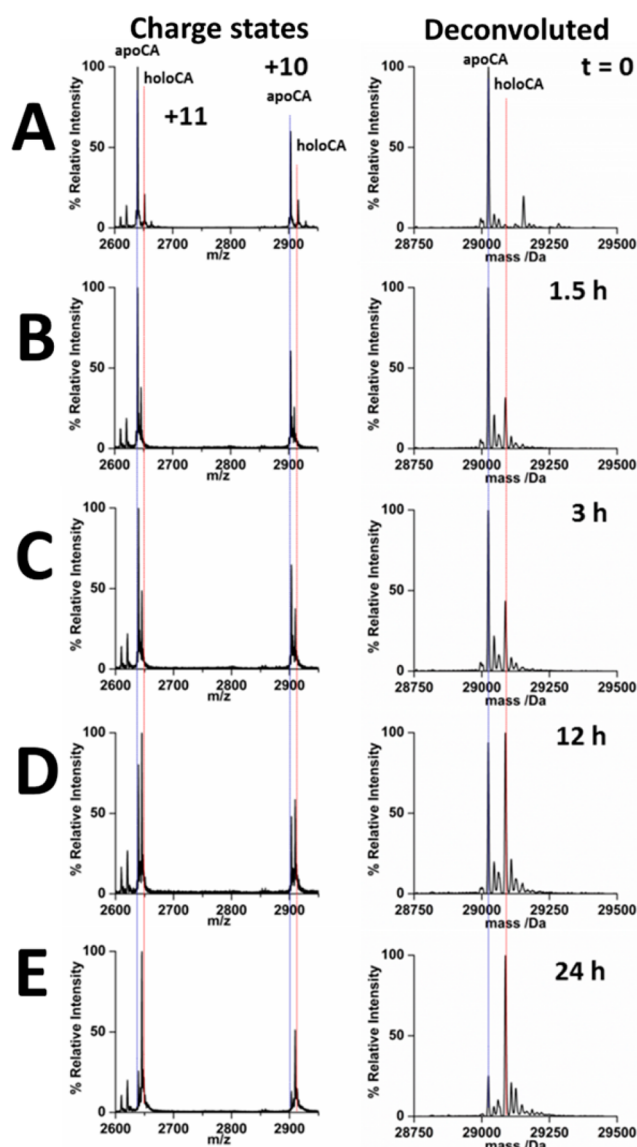


Figure 1. (A–E) Time dependence of the CA metalation by Zn₇-MT. Representative ESI mass spectral data for CA measured during the reaction between 15 μM apoCA and 12 μM Zn₇-MT are shown. The +10 and +11 charge states of CA are shown on the left, and the corresponding deconvoluted mass are on the right. The conditions of the reaction were 5 mM ammonium formate, pH 7.0 buffer, 25 °C.

shown on the left, and the corresponding reconstructed deconvoluted masses are on the right. At the start of the reaction, the CA is almost completely in the apo form, with no detected Zn-CA in either the charge states or the deconvoluted spectra (Figure 1A), demonstrating the near complete extraction of zinc from Zn-CA by the zinc removal procedure. Figure 1B–E shows an increase in Zn-CA levels as the apoCA is metalated by the Zn-MT. The apoCA is only approximately 50% metalated after 12 h of reaction time (Figure 1D) and is still not 100% metalated by 24 h (Figure 1E).

The complementary data for MT are shown in Figure 2. However, far more details can be extracted from these data. The speciation of the MT is complicated by the multiple metalation states that coexist in solution. At the start of the experiment, the MT is mostly Zn₇-MT with a small amount of Zn₆-MT and approximately 0.5 equiv (per mol equiv of total metal binding sites) of cadmium remaining from the

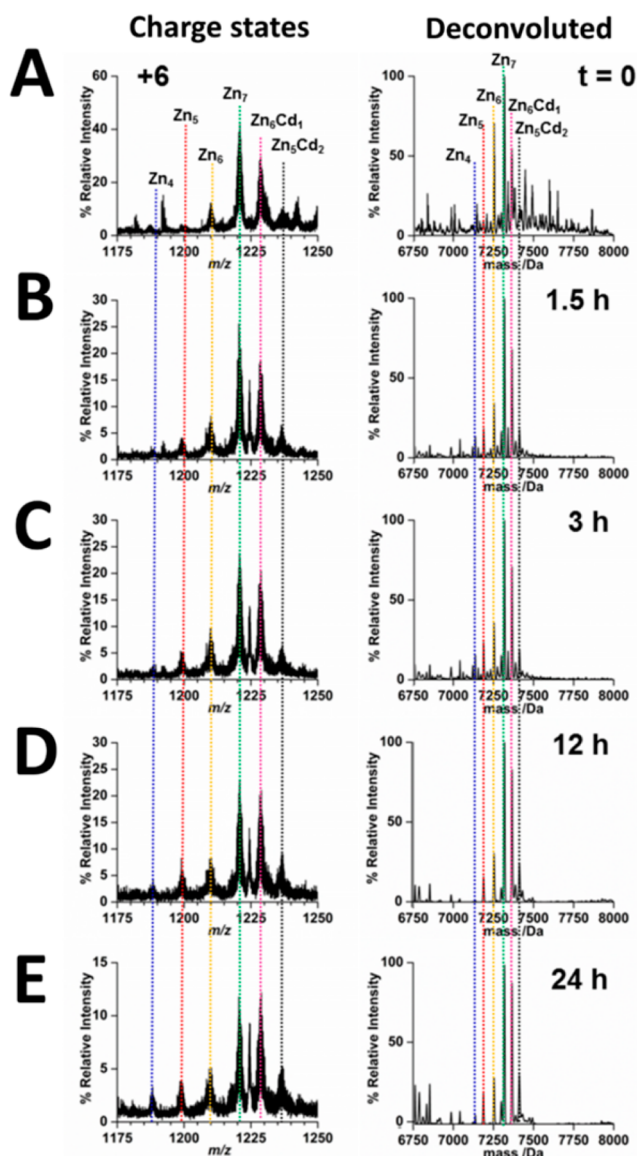


Figure 2. (A–E) Time dependence of the $\text{Zn}_7\text{-MT}$ demetalation by apoCA. Representative ESI mass spectral data for MT measured during the reaction between $15\ \mu\text{M}$ apoCA and $12\ \mu\text{M}$ $\text{Zn}_7\text{-MT}$. The +6 charge state of MT is shown on the left, and the corresponding deconvoluted mass is on the right. There is a trace contamination of cadmium that appears unaffected by the exchange of zinc from MT to CA. The conditions of the reaction were $5\ \text{mM}$ ammonium formate, pH 7.0 buffer, $25\ ^\circ\text{C}$.

purification and metal exchange procedures (Figure 2A) that does not appear to participate in the metal exchange reaction with apoCA (as described below). As the reaction proceeds, the $\text{Zn}_6\text{-MT}$ signal intensifies and $\text{Zn}_5\text{-MT}$ appears after 1.5 h (Figure 2B). There is a general buildup of signal intensity for $\text{Zn}_{4-6}\text{-MT}$ over the duration of the experiment, with a corresponding decrease in $\text{Zn}_7\text{-MT}$. Significantly, no $\text{Zn}_3\text{-MT}$ was detected in either the charge state or deconvoluted spectra.

To compare the changes in speciation as a function of time, the relative peak intensities were extracted from the deconvoluted data and plotted as a function of time for the MT (Figure 3A) and CA (Figure 3B) species. The change in MT speciation over time shows that there is fast transfer from $\text{Zn}_7\text{-MT}$, followed by much slower release from $\text{Zn}_6\text{-}$ and $\text{Zn}_5\text{-}$

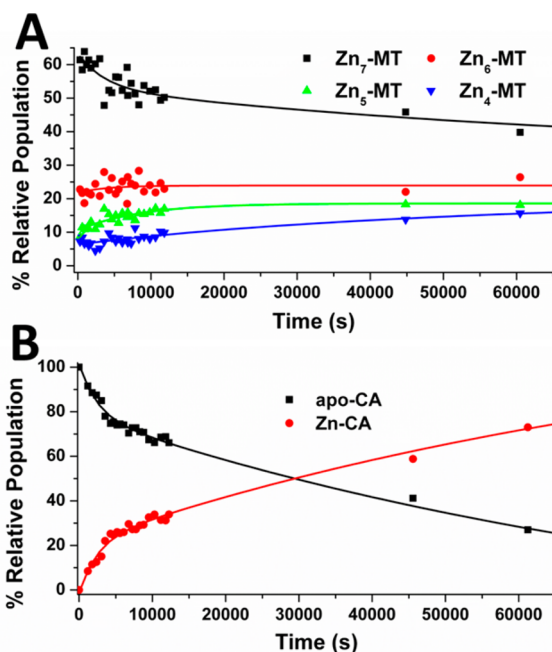


Figure 3. Time courses of the demetalation of (A) Zn-MT and the metalation of (B) apoCA extracted from the ESI mass spectral data shown in Figures 1 and 2. The lines have been added to guide the eye.

MT. In fact, the $\text{Zn}_6\text{-}$ and $\text{Zn}_5\text{-MT}$ speciation traces only reached steady states after 10 000 s. Figure 3A extracts the individual populations of the four key MT species. The overall reaction is $\text{Zn}_7\text{-MT} \rightarrow \text{Zn}_6\text{-M} \rightarrow \text{Zn}_5\text{-MT} \rightarrow \text{Zn}_4\text{-MT}$, with each step donating a zinc to the apoCA. The equilibrium data we previously published showed that at this metalation point, these three partially demetalated species would coexist.²⁵ Figure 3A shows the change in speciation population as each of these partially metalated species equilibrates over time. The complexity in the figure derives from the presence of all four MT species in the mass spectral data.

Figure 3B shows the corresponding time course for the CA speciation. Because there is only one zinc bound, the data are significantly less complicated. At the 80 000 s data point only 80% of the CA had metalated, despite the fact that there were still significant amounts of $\text{Zn}_7\text{-MT}$ and $\text{Zn}_6\text{-MT}$ in solution.

Pseudo-second order kinetic analysis, based on assumption that all of the zinc that was bound by the apoCA was originally bound in Zn-MT , is shown in Figure 4. The plot shows a strong correlation to the linear fit of the data, especially for the early phase of the reaction. The second order rate constant, first order in apoCA and first order in Zn-MT , determined from the slope was $2.5 \pm 0.5\ \text{M}^{-1}\ \text{s}^{-1}$.

Kinetics of the Reaction between $\text{Zn}_7\text{-MT}$ and Cd-CA . Metal exchange between $30\ \mu\text{M}$ $\text{Zn}_7\text{-MT}$ and $30\ \mu\text{M}$ Cd-CA was measured continuously using ESI-MS. The peak intensities were extracted from the deconvoluted spectra of the data as described in the Methods. The speciation time course curves of MT show the successive reactions of $\text{Zn}_7\text{-MT}$ with Cd-CA forming $\text{Zn}_6\text{Cd}_1\text{-MT}$ which can react with another equivalent of Cd-CA to give $\text{Zn}_5\text{Cd}_2\text{-MT}$. The time course for these reactions, from the ESI mass spectral data measured over 30 000 s, is shown in Figure 5, panels A and B, respectively.

The only MT species that were detected in the ESI mass spectral data were the metal saturated forms $[(\text{M}^{\text{II}})_7\text{-MT}]$, as mixtures of zinc and cadmium [e.g., $n(\text{Zn}^{2+}) + m(\text{Cd}^{2+}) = 7$].

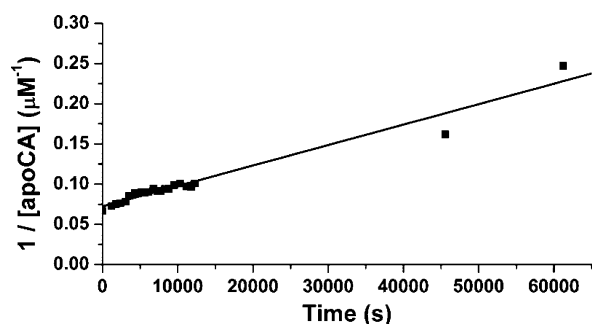


Figure 4. Second order kinetic analysis of the zinc metalation of apoCA under MT limiting conditions. The line is based on the speciation trace shown in Figure 3, assuming that the reacting species were at equal concentration, and $[\text{apoCA}]_{t=0} = 15 \mu\text{M}$. The apparent second order rate constant for the reaction under these conditions, as determined from a linear regression of the data, is $2.5(4) \pm 0.5(3) \text{ M}^{-1} \text{ s}^{-1}$.

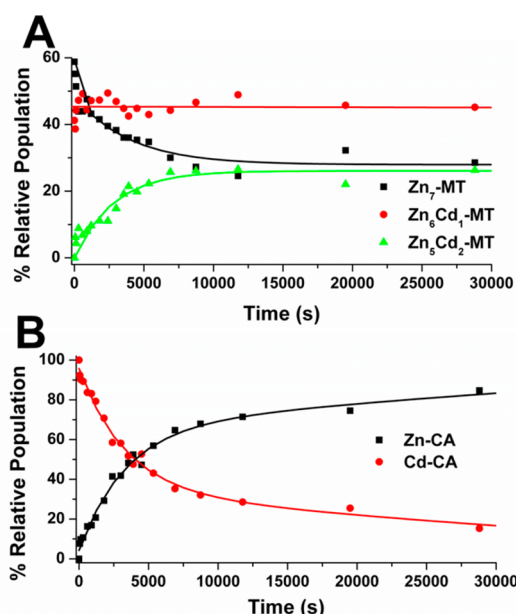


Figure 5. Time course of the metal exchange between $\text{Zn}_7\text{-MT}$ and Cd-CA. (A) MT and (B) CA. Species were extracted from the ESI mass spectral data of the reaction between an equimolar ($30 \mu\text{M}$) mixture of Cd-CA and $\text{Zn}_7\text{-MT}$. The lines have been added to guide the eye. Conditions: 5 mM ammonium formate, pH 7.0, 37°C .

Initially, the reaction begins with zinc saturated $\text{Zn}_7\text{-MT}$, which exchanges one zinc for a cadmium bound in Cd-CA to form $\text{Cd}_1\text{Zn}_6\text{-MT}$. This species reacts with another Cd-CA to form $\text{Cd}_2\text{Zn}_5\text{-MT}$. No other cadmium containing species were observed in either the charge state or deconvoluted mass spectra. The trend in the $\text{Zn}_6\text{Cd}_1\text{-MT}$ population reflects the equilibrium between $\text{Zn}_7\text{-MT}$ and $\text{Zn}_5\text{Cd}_2\text{-MT}$ where the trafficking of the zinc to the CA in response to the change due to cadmium binding to the MT results in a near constant population for $\text{Zn}_6\text{Cd}_1\text{-MT}$.

The corresponding CA metalation time course is more straightforward, which is reflective of the simpler one-for-one exchange of cadmium for zinc over the course of the reaction. The zinc from the Zn-MT [$\log(K_{\text{Zn-MT}} = 11.5)$, $\log(K_{\text{Cd-MT}} = 14)$] is exchanging with the cadmium initially bound as Cd-CA [$\log(K_{\text{Cd-CA}} = 11.1$ vs $\log(K_{\text{Zn-CA}} = 12.0)$] favorably because of the thermodynamically preferred metal substitution. Again,

only 80% of the Cd-CA exchanges with Zn-MT by 30 000 s despite the fact that significant amounts of exchangeable zinc ($\text{Zn}_7\text{-MT}$) are available.

The integrated, pseudo-second order rate plot of $1/[\text{Cd-CA}]$ vs t , for the reaction between $\text{Zn}_7\text{-MT}$ and Cd-CA and based on assumptions regarding the kinetics of the reaction described in detail in the Methods and above, shows a good correlation to the linear fit of the data (Figure 6). We determined the second order rate constant (first order in Cd-CA and first order in Zn-MT) for the reaction of Cd-CA with Zn-MT at 37°C to be approximately $6.0 \text{ M}^{-1} \text{ s}^{-1}$.

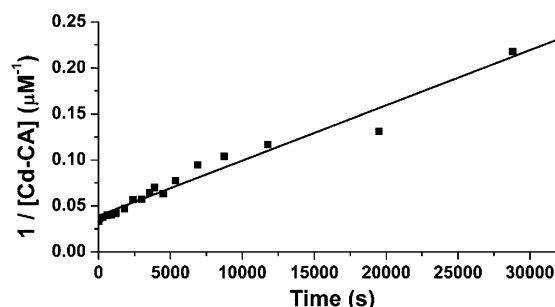


Figure 6. Second order kinetic analysis of the reaction of Cd-CA with $\text{Zn}_7\text{-MT}$. The line is based on the speciation trace (loss of Cd-CA) shown in Figure 5 and $[\text{Cd-CA}]_{t=0} = 30 \mu\text{M}$. The apparent second order rate constant for the reaction under these conditions, as determined from the linear regression of the data, is $6.0(0) \pm 0.5(8) \text{ M}^{-1} \text{ s}^{-1}$.

Kinetics of the Reaction between Partially Metalated Zn-MT and Cd-CA.

We investigated the effect of unoccupied metal binding sites in the MT on the reaction between partially metalated Zn-MT and Cd-CA. Thirty micromolar Cd-CA was mixed with $30 \mu\text{M}$ unsaturated Zn-MT at 37°C , and the cadmium–zinc exchange reaction was monitored continuously using ESI-MS. The mass spectral data (not shown) indicated that the MT initially existed as a mixture of Zn_{3-6}MT , with Zn_4 - and Zn_5 - being the most populated MT metalated states. Thus, at the start of the reaction there was a mixture of between one and four unoccupied metal binding sites, with an average of between two and three unoccupied binding sites per MT protein.

The time course for the change in the population of all of the MT species extracted from the deconvoluted ESI mass spectral data for this reaction is shown in Figure 7A. This figure shows the change in the relative speciation of all of the detected MT species as a function of reaction time and highlights the complexity of reactions involving multiple species. The data show that the $\text{Zn}_4\text{-MT}$ species remains approximately constant as a result of the net balance of all of the reactions that consume or produce $\text{Zn}_4\text{-MT}$: $\text{Zn}_5\text{-MT} \rightarrow \text{Zn}_4\text{-MT} + \text{Zn}^{2+}$; $\text{Zn}_4\text{-MT} \rightarrow \text{Zn}_3\text{-MT} + \text{Zn}^{2+}$; $\text{Zn}_4\text{-MT} + \text{Cd}^{2+} \rightarrow \text{Zn}_4\text{Cd}_1\text{-MT}$. The change in the populations for each of the other MT species shown in Figure 7A is also the net sum of the set of reactions involving that species.

Overall, the cadmium content of the MT species increases over the course of the reaction and the zinc content decreases. This trend is more easily observed in Figure 7B, where the ratio of $\text{Cd}_1\text{Zn}_{n-1}\text{-MT}/\text{Zn}_n\text{-MT}$ has been plotted as a function of reaction time in order to compare the change in cadmium content per metalation state (i.e., each line represents the change in cadmium content for $(\text{M}^{\text{II}})_{4-6}\text{-MT}$). For example,

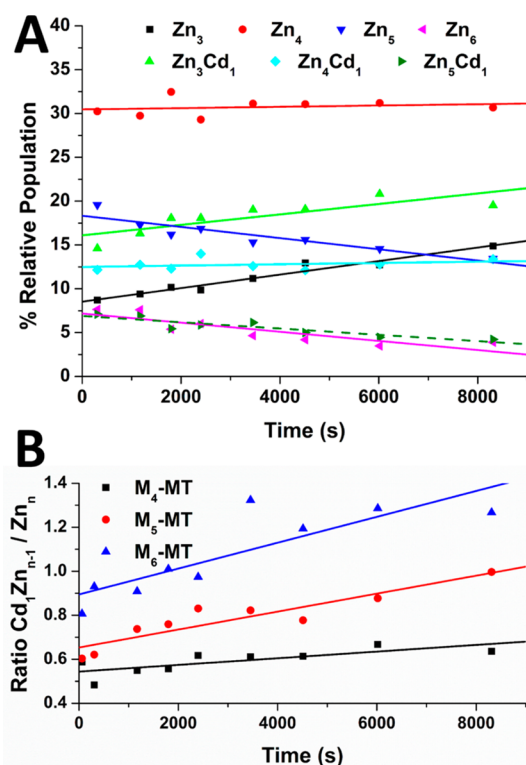


Figure 7. Time dependence of the populations of metallothionein species for the reaction between partially metalated Zn-MT and Cd-CA. (A) Experimentally determined time courses of MT species extracted from the ESI mass spectral data of the reaction between an equimolar ($30 \mu\text{M}$) mixture of Cd-CA and $Zn_{(3-6)}$ -MT (average zinc = 4.5). Conditions: 5 mM ammonium formate, pH 7.0, 37°C . (B) Trend in the ratio of $CdZn_{(n-1)}$ -MT/ Zn_n -MT for the values of $n = 4-6$. The trends in the data show the change in cadmium occupancy for each of the detected species as a function of time. The lines are based on linear fits to the data.

the positive slope of the blue line (Zn_5Cd_1 -MT/ Zn_6 -MT) shows that the Zn_5Cd_1 -MT population is increasing relative to the population of Zn_6 -MT. Each of the lines shown in Figure 7B, therefore, shows the increasing cadmium fraction in the three MT metalation states [$(M^{II})_{4-6}$ -MT] over the duration of the reaction. As these lines originate from the respective trends shown in Figure 7A, the magnitudes of the slopes of the lines in Figure 7B are not normalized and are, therefore, not comparable with each other.

The corresponding time course for the CA speciation during the reaction with the partially metalated Zn-MT is shown in Figure 8. The data show that initially all of the CA was of the cadmium bound form. Notably the apoCA did not extract the zinc from the partially metalated Zn-MT presumably because the zinc loading of the MT was only Zn_{3-6} -MT to begin with. Thus, the formation of the apoCA, formed from extraction of cadmium by the unoccupied MT sites, which have larger cadmium affinity values, occurs at about an order of magnitude faster than formation of the Zn-CA.

The disappearance of the Cd-CA was plotted as a pseudo-second order reaction (first order with respect to CA and to MT), and the results of the analysis are shown in Figure 9. The data show strong correlation to a linear fit that determined the second order rate constant as approximately $11.7 \text{ M}^{-1} \text{ s}^{-1}$, from the slope of the line in Figure 9. This rate is approximately

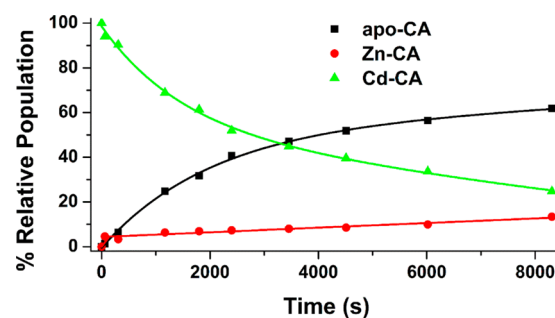


Figure 8. Experimentally determined time courses of CA species extracted from the ESI mass spectral data of the reaction between an equimolar ($30 \mu\text{M}$) mixture of Cd-CA and $Zn_{(3-6)}$ -MT. Conditions: 5 mM ammonium formate, pH 7.0, 37°C . The lines have been added to guide the eye.

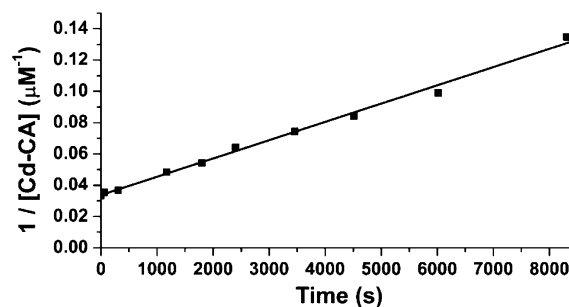


Figure 9. Second order kinetic analysis of the reaction of Cd-CA with partially zinc metalated MT. The line is based on the speciation trace (loss of Cd-CA) shown in Figure 8 and $[Cd-CA]_{t=0} = 30 \mu\text{M}$. The apparent second order rate constant for the reaction under these conditions, as determined from the linear regression of the data, is $11.6(8) \pm 0.7(2) \text{ M}^{-1} \text{ s}^{-1}$.

twice as fast as that determined for the reaction between zinc saturated MT and Cd-CA at the same temperature (Figure 6).

DISCUSSION

The report of a cadmium-specific carbonic anhydrase (CDCA) from *Thalassiosira weissflogii* microalgae was the first to demonstrate a native catalytically active role for cadmium.¹⁹ This protein was discovered and subsequently purified and crystallized under extremely zinc-limiting conditions. Unlike mammalian CAs, CDCA was shown to have a higher affinity for cadmium than for zinc, possibly due to differences in the binding site ligands. Metal exchange experiments between CDCA and zinc or cadmium phytochelatins (Pc) showed faster rates of exchange compared to zinc or cadmium chelated to nitrilotriacetic acid (NTA).²⁰ Those results parallel the ones in this report where we examine the effects of limiting zinc on similar exchange experiments between the mammalian partners, namely, Zn-MT and Cd-CA.

Protein–Protein Interactions (PPIs) between Metallothionein and Other Metal Binding Sites. Evidence of PPIs between MTs and metalloenzymes comes mostly from reports of the zinc donation properties of Zn_7 -MT to apo-zinc-dependent proteins.^{26–28} There have been two very significant reports of metal substitution between MTs and cadmium-substituted zinc-dependent enzymes. In the first report, Zn_7 -MT was shown to exchange a single zinc for the cadmium bound to the zinc finger domain of the Tramtrack transcriptional repressor protein.²⁹ The second report investigated the

kinetics of the metal exchange between apo and Zn₇-MT and cadmium-substituted bovine carbonic anhydrase (Cd-CA) where the apoMT extracted the cadmium from Cd-CA over 20× faster than the Zn₇-MT exchange reaction.³⁰

Most reported studies between Zn-MT and zinc binding proteins use an excess of Zn-MT as the zinc source. Therefore, those results are only largely descriptive of the reactions involving Zn₇-MT, since it is in excess, and not the partially metalated species. Previously, our group and others have demonstrated that there are seven different zinc binding affinities of MTs, and thus the metal affinity for an incoming metal depends on the metal loading.^{25,31} Each of the reactions of Zn_n-MTs (where $n = 0-6$) for either zinc donation or cadmium exchange is controlled by different reaction parameters. This is important because there is evidence of substantial pools of partially metalated MTs *in vivo* which means that these partially metalated MTs play a key role in MT's function.³²

Metal Binding to Carbonic Anhydrase. Zinc and cadmium are bound in mammalian CA tetrahedrally by three HIS and a labile water molecule. Significantly, CA binds zinc and cadmium with similar affinities of approximately ($\log_{10}(K_F)$) 12.0 and 11.1, respectively at pH 7.0.³³ The pH 7.0 zinc binding affinity has more recently been suggested to fall even closer (11.4) to that reported for cadmium.³⁴ Thus, the ratio of the binding constants K_F^{Cd}/K_F^{Zn} is small compared with the same ratio for MT, and there is, therefore, no significant driving force for metal exchange in CA. This means that CA with an existing cadmium or zinc in its binding site is resistant to exchange with free metal in solution as has been demonstrated for many metals where similar exchanges involving free metals were shown to take from days to weeks.^{35,36}

Free metals added to the apoCA protein bind rapidly. For example, in both zinc and cadmium titration experiments of apoCA, metal binding occurs within the time of ESI mass spectral data acquisition (<10 s) following stoichiometric mixing (data not shown). However, *in vivo*, metal concentrations are tightly regulated, and the concentrations of free metals are far below that which would support free metal association to apoenzymes following their transcriptional synthesis. Therefore, other zinc sources and chaperones must deliver and insert the zinc into these active sites, as suggested as a function of Zn-MTs.²⁸

With the goal of obtaining more details regarding the role of Zn-MTs in reactions with metalloenzymes, we have investigated a series of metal exchange reactions between Zn-MTs and CA. We used CA as a putative zinc-binding protein. The above results describe the metalation statuses of both the MT and CA species as a function of time.

Are the Zinc Donation Kinetics Different for Partially Metalated MTs? In Figure 3, the latter stages of the metal transfer reaction between Zn-MTs and apoCA, when a significant fraction of the apoCA is metalated and there is less apoCA to donate to, the Zn₇-MT → Zn₆-MT → Zn₅-MT → Zn₄-MT reactions occur at approximately the same rate such that the rate of formation of Zn₄-MT approximately matches the rate of loss of Zn₇-MT. We interpret this result as due to the redistribution of zinc in the MT species, restoring the thermodynamically preferred zinc occupancy based on the zinc affinities of the different Zn_n-MT species following a zinc donation event from Zn₅₋₇-MT to apoCA.

These data match the results from the competitive titration between apoMT and apoCA for added zinc under equilibrium conditions.³⁷ The apoCA was shown to only compete effectively with Zn₅₋₇-MT and not with Zn₁₋₄-MT. In another set of experiments, where the ratio of apoCA:Zn₃Cd₄-MT was 7:1, only 1.4 zincs were released by the MT, though further zinc donation was initiated by incubating in the presence of GSH and GSSG.³⁸

When the Zn₇-MT was in excess, Figure 3, meaning that the majority of the donated zinc species would be from Zn₇-MT → Zn₆-MT, the zinc donation kinetics were faster. For example, in time course experiments between excess Zn₇-MT and apoCA, also studied by ESI-MS, the apoCA was 50% metalated within 2400 s (conditions: 10 mM ammonium acetate, pH 7.5, unknown temp.).²⁷ This is over 10× faster than the reaction shown here, Figure 3B, where the apoCA is 50% metalated after 25 000 s.

In conclusion, the zinc donation properties of Zn-MTs are modulated by the binding affinity differences between the zinc donor and the zinc acceptor. The thermodynamics (and kinetics) favor zinc donation more strongly the greater the binding affinity difference is between the zinc donor and the zinc acceptor, and the reaction occurs faster as well. We now know that the zinc are bound to MT with differing affinities [values range from $\log(K_F)$ 12.5 to 11.8],²⁵ and we thus expected to see slower zinc donation kinetics for Zn_n-MTs ($n < 7$). Comparing these new data to those available in the literature, we have shown that Zn₅- and Zn₆-MTs donate much more slowly than Zn₇-MTs. These results support the model of Zn₇-MT and Zn₆-MT as the most probable source of MT zinc donation to CA. Other zinc-binding sites will “extract” zinc from Zn_n-MT relative to the zinc binding affinity difference between the zinc acceptor (the empty site) and donor (the Zn_n-MT).

How Readily Does Zinc Saturated MT Exchange with Cd-CA? Cadmium detoxification is another commonly described *in vivo* function of Zn-MTs. Several studies have shown that cadmium binds to MTs via very fast reaction, often within the dead-time of stopped-flow instruments (<10 ms), using free cadmium as the Cd source.^{16,39} These reactions are significantly slowed when the cadmium is bound by another chelator, such as another protein.⁴⁰ The metal exchange reactions are reflective of the relative binding affinities for cadmium and zinc between the two binding sites, i.e., the difference between the metal preferences of one site vs another. For example, in the case of Cd-CA mixed with Zn-MT, the metal exchange will depend on the magnitude of $((K_{CA_{Zn}})/(K_{CA_{Cd}})) \cdot ((K_{MT_{Cd}})/(K_{MT_{Zn}}))$. CA binds zinc with a higher affinity than cadmium, and MT binds cadmium with a higher affinity than zinc; this ratio is largely positive and a favorable exchange is predicted to occur, thermodynamically. Additionally, cadmium and zinc each bind to MT and CA with relatively high affinities and therefore small dissociation constants, $K_d < 10^{-11}$. Thus, only very small concentrations of free cadmium or free zinc would be in a solution containing MT and CA, and the rate of the exchange, for a dissociative-associative metal exchange mechanism would be extremely slow.

The population time course data for the MT species (Figure 5A) show that there is an initial rapid Zn₇-MT to Cd₁Zn₆-MT reaction, most likely due to a small excess of cadmium that was nonspecifically bound to the exterior of the Cd-CA protein. This is followed by a slower reaction of Cd₁Zn₆-MT forming

$\text{Cd}_2\text{Zn}_5\text{-MT}$. The intermediate $\text{Cd}_1\text{Zn}_6\text{-MT}$ reaches approximately a steady state within the first 2000 s, after which, formation from $\text{Zn}_7\text{-MT}$ matches the rate of the reaction that forms $\text{Cd}_2\text{Zn}_5\text{-MT}$.

The CA speciation (Figure 5B) shows a similar trend in the change in speciation over the reaction time. The initial zinc exchange for the bound cadmium, from primarily $\text{Zn}_7\text{-MT}$ (up to 2000 s), appears to occur at a faster rate than later in the reaction (where the pool of MT contains more cadmium and the Cd-CA would also encounter $\text{Cd}_1\text{Zn}_6\text{-MT}$). Interestingly, even up to almost 30 000 s, a significant fraction of the Cd-CA remains, despite the fact that there are zinc ions available for donation from the MT ($\text{Zn}_7\text{-MT}$ and $\text{Cd}_1\text{Zn}_6\text{-MT}$). We interpret this to indicate that the reaction is approaching equilibrium, where the average relative affinity constants for zinc and cadmium binding to MT are approaching equality to those for CA, with respect to the concentrations of each of the species in solution.

This second order rate constant determined here of $6.0 \text{ M}^{-1} \text{ s}^{-1}$ at 37°C is faster than that reported in the literature by Ejnik et al. where they reported a value of $2.3 \text{ M}^{-1} \text{ s}^{-1}$ at the same temperature.³⁰ The approximate agreement between these two values, however, verifies that the experimental design and data analysis procedures are accurately reflecting the kinetics of these (and similar) reactions. We also attempted to measure the kinetics at 25°C , but we observed no metal exchange reaction, up to 18 h ($\sim 65\,000 \text{ s}$). This result also matches those report by Ejnik et al. where the second order reaction rate constant ($0.33 \text{ M}^{-1} \text{ s}^{-1}$) was almost $7\times$ slower at the colder temperature.³⁰

In conclusion, $\text{Zn}_7\text{-MT}$ is able to efficiently exchange bound zinc for bound cadmium from Cd-CA . Because the rate of the reaction between the Zn-MT and Cd-CA occurs much more rapidly than is possible for a dissociative–associative metal exchange mechanism, these results support the PPI model of metal exchange between MT and enzymes.

Are the Metal Exchange Kinetics between Cd-CA and $\text{Zn}_{(3-5)}\text{-MTs}$ Faster or Slower Compared to Those for $\text{Zn}_7\text{-MT}$? The results from the previous set of experiments raise an interesting question: if all the metal binding sites in the MT-CA complex are occupied, how does the metal exchange take place? Since there are no obvious metal binding ligands that are free in the MT, and the CA active site is prefilled with cadmium, the exchange must somehow take place within the MT-CA complex. Significantly, Nettesheim et al. showed that MTs are able to exchange cadmium and zinc between fully metalated MT strands without the intermediacy of free metal ions.⁷ With open metal binding sites in either the CA or MT, the metal exchange may become easier because the lability of the metals allows for the use of free thiolate ligands to facilitate the exchange process.

The speciation time courses in Figure 7 are complicated by the overlap of two competing processes: the binding of cadmium, which increases the metal load per MT, is competing against the zinc donation to the apoCA which decreases the metal loading. As discussed above, the metal donation properties of partially metalated MTs differs significantly depending on the number of zincs bound. Thus, the time courses in Figure 7 are each the sum of the reactions that bind cadmium and donate zinc. Looking only at the zinc metalation species, we see a decrease in the $\text{Zn}_6\text{-}$ and $\text{Zn}_5\text{-MT}$ speciation over the course of the reaction and a significant increase in $\text{Zn}_3\text{-MT}$ population.

The time course data corresponding to the CA species (Figure 8) clearly show how under these conditions, the metal exchange between Cd-CA and $\text{Zn}_n\text{-MT}$ occurs via a two-step mechanism. The first step is the relatively fast extraction of cadmium from the Cd-CA into the empty metal binding sites in the partially metalated Zn-MTs . The second step is the relative slow release of zinc from the partially metalated Zn-MTs to the now available apoCA from the previous step. It is important to note that the rates of these two steps will be dependent on the metal loading status of the MT; more empty metal binding sites will extract cadmium faster, while MTs with more zinc will donate zinc faster.

These results support the hypothesis that an open coordination site results in faster cadmium extraction from a cadmium-substituted zinc enzyme. The second order rate constant obtained here ($11.2 \text{ M}^{-1} \text{ s}^{-1}$) is slower than that reported by Ejnik et. al of $18.2 \text{ M}^{-1} \text{ s}^{-1}$ for the reaction between apoMT and CdCA also measured at 37°C .³⁰ Significantly, the second order rate constant for the partially metalated MTs ($\sim 11 \text{ M}^{-1} \text{ s}^{-1}$) falls between that of zinc saturated MT ($\sim 6 \text{ M}^{-1} \text{ s}^{-1}$) and apoMTs ($\sim 18 \text{ M}^{-1} \text{ s}^{-1}$), which is a reflection of the cadmium-extraction abilities of each of the MT species.

Structure of CA and Relevance to PPIs with MT. The crystal structure of carbonic anhydrase II shows that the three His active site sits at the bottom of a cavity that is approximately $10\text{--}20 \text{ \AA}$ across and $15\text{--}20 \text{ \AA}$ deep (Figure 10). This cavity is large enough to allow amino acid side chains from the MT to approach the metal binding site, especially for a Cys side chain within a flexible loop.

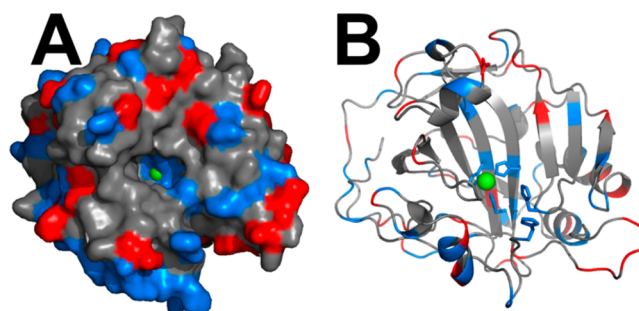


Figure 10. X-ray crystal structure of CA and metal binding residues that could facilitate metal transfers. Structure of human erythrocyte carbonic anhydrase II (1CA2)⁴¹ showing (A) the surface and active site and (B) the cartoon representation. The residues have been colored according to charge: red = negatively charged, blue = positively charged. The zinc in the active site is shown as a green sphere.

In the MT-CA complex, nearby metal binding residues along the metal exchange pathway may facilitate the metal exchange process. The structure of CA shows that there are two histidines that would be well suited to assist in the zinc delivery or cadmium removal as intermediate metal binding residues in the exchange process. His4 sits on the rim of the active site funnel and His64 sits approximately halfway down the length of the funnel (Figure 10B, right of the zinc binding site). Other features of the CA protein that would be favorable to PPIs with MT are the presence of multiple surface charges that could form electrostatic interactions with the MT as shown in Figure 11.

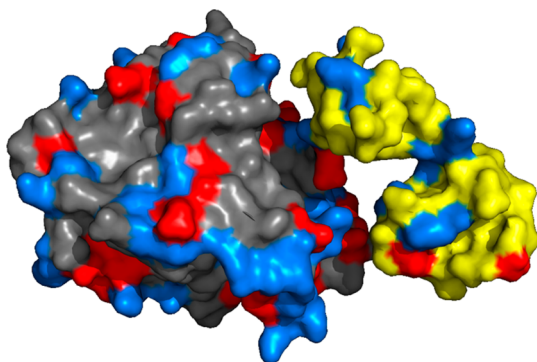


Figure 11. Manual docking of the crystal structures of CA and MT. CA (1CA2)⁴¹ and MT (4MT2)⁵ electrostatic contacts near the active site of the CA are able to align well with complementary charged residues of MT. The cavity size outside of the active site also permits close approach of the MT protein.

CONCLUSIONS

The metal donation properties of metallothioneins have been well studied, yet many questions remain. Initially MTs were identified as having solely toxicological action from the reports of binding toxic metal ions. More recently, MTs have been suggested to play roles in the essential metal ion homeostasis of zinc and copper. The true function of MTs *in vivo* are likely a combination of the toxic metal detoxification and essential metal homeostasis, depending on the cellular metalation status (a role in cellular redox chemistry has also been suggested).

In this work, we have investigated the role of partially metalated MTs in zinc donation to an apo-zinc-dependent enzyme, carbonic anhydrase. We showed that partially metalated MTs donate zinc with different propensities as a direct result of the relative binding affinities of each Zn_n-MT species for its bound zinc ions. These results support our current model where Zn₇- and Zn₆-MT are the primary zinc donating species for Zn-MTs.

We have also shown that partially metalated MTs are able to extract cadmium at rates intermediate to apoMT (fastest) and zinc saturated MT (slowest) as a function of the number of open metal binding sites. These results suggest that metal exchange occurs in two separate steps where cadmium removal from Cd-CA occurs first, followed by a slow binding of zinc from the Zn-MT. Taken together, the results from this work support a model for metal transfers between MT and other proteins that is via protein–protein interactions which permit the essential metal homeostatic and toxic metal sequestration roles of MTs *in vivo*.

With respect to a native mammalian cadmium-containing CA, our results suggest that even under zinc-limiting conditions, the cadmium in Cd-CA would be rapidly bound by the MT and that under more extreme zinc limiting conditions that the MT would not donate zinc to apoCA, a situation not reported for CDCA.

AUTHOR INFORMATION

Corresponding Author

*Phone: (519) 661-3821. Fax: (519) 661-3022. E-mail: martin.stillman@uwo.ca.

Funding

Research funded by Natural Sciences and Engineering Research Council of Canada

Notes

The authors declare no competing financial interest.

ACKNOWLEDGMENTS

We thank Mr. Doug Hairsine for excellent technical support and advice on the operation of our mass spectrometers. We acknowledge financial support from the Natural Sciences and Engineering Research Council of Canada for Discovery and RTI grants (to M.J.S.) as well as a graduate scholarship (to T.B.J.P.).

ABBREVIATIONS

apoCA, metal-free carbonic anhydrase; apoMT, metal-free metallothionein; CA, mammalian carbonic anhydrase; Cd-CA, mammalian cadmium substituted carbonic anhydrase; CDCA, cadmium-specific carbonic anhydrase from *Thalassiosira weissflogii*; ESI-MS, electrospray ionization mass spectrometry; K_F , formation constant; MT, mammalian metallothionein; MT1A, human metallothionein 1A isoform; MWCO, molecular weight cutoff; PPI, protein–protein interactions

REFERENCES

- (1) Kang, Y. J. (2006) Metallothionein redox cycle and function. *Exp. Biol. Med.* 231, 1459–1467.
- (2) Maret, W., and Vallee, B. L. (1998) Thiolate ligands in metallothionein confer redox activity on zinc clusters. *Proc. Natl. Acad. Sci. U. S. A.* 95, 3478–3482.
- (3) Sabolić, I., Breljak, D., Škarica, M., and Herak-Kramberger, C. M. (2010) Role of metallothionein in cadmium traffic and toxicity in kidneys and other mammalian organs. *BioMetals* 23, 897–926.
- (4) Maret, W. (2000) The function of zinc metallothionein: a link between cellular zinc and redox state. *J. Nutr.* 130, 1455S–1458S.
- (5) Braun, W., Vasak, M., Robbins, A., Stout, C., Wagner, G., Kägi, J., and Wüthrich, K. (1992) Comparison of the NMR solution structure and the X-ray crystal structure of rat metallothionein-2. *Proc. Natl. Acad. Sci. U. S. A.* 89, 10124–10128.
- (6) Nielson, K. B., Atkin, C., and Winge, D. (1985) Distinct metal-binding configurations in metallothionein. *J. Biol. Chem.* 260, 5342–5350.
- (7) Nettesheim, D. G., Engeseth, H. R., and Otvos, J. D. (1985) Products of metal exchange reactions of metallothionein. *Biochemistry* 24, 6744–6751.
- (8) Hinkle, P. M., Kinsella, P., and Osterhoudt, K. (1987) Cadmium uptake and toxicity via voltage-sensitive calcium channels. *J. Biol. Chem.* 262, 16333–16337.
- (9) Waalkes, M. P., and Goering, P. L. (1990) Metallothionein and other cadmium-binding proteins: recent developments. *Chem. Res. Toxicol.* 3, 281–288.
- (10) Bertin, G., and Averbeck, D. (2006) Cadmium: Cellular effects, modifications of biomolecules, modulation of DNA repair and genotoxic consequences (a review). *Biochimie* 88, 1549–1559.
- (11) Andrews, G. K., Lee, D. K., Ravindra, R., Lichtlen, P., Sirito, M., Sawadogo, M., and Schaffner, W. (2001) The transcription factors MTF-1 and USF1 cooperate to regulate mouse metallothionein-I expression in response to the essential metal zinc in visceral endoderm cells during early development. *EMBO J.* 20, 1114–1122.
- (12) Langmade, S. J., Ravindra, R., Daniels, P. J., and Andrews, G. K. (2000) The transcription factor MTF-1 mediates metal regulation of the mouse ZnT1 gene. *J. Biol. Chem.* 275, 34803–34809.
- (13) Durnam, D., and Palmiter, R. (1981) Transcriptional regulation of the mouse metallothionein-I gene by heavy metals. *J. Biol. Chem.* 256, 5712–5716.
- (14) Mayo, K. E., Warren, R., and Palmiter, R. D. (1982) The mouse metallothionein-I gene is transcriptionally regulated by cadmium following transfection into human or mouse cells. *Cell* 29, 99–108.

- (15) Squibb, K. S., Cousins, R. J., and Feldman, S. L. (1977) Control of zinc-thionein synthesis in rat liver. *Biochem. J.* 164, 223–228.
- (16) Ejnik, J., Robinson, J., Zhu, J., Försterling, H., Shaw, C. F., and Petering, D. H. (2002) Folding pathway of apo-metallothionein induced by Zn^{2+} , Cd^{2+} and Co^{2+} . *J. Inorg. Biochem.* 88, 144–152.
- (17) Ejnik, J., Shaw, C. F., III, and Petering, D. H. (2010) Mechanism of cadmium ion substitution in mammalian zinc metallothionein and metallothionein α domain: kinetic and structural studies. *Inorg. Chem.* 49, 6525–6534.
- (18) Laskowski, R. A., Luscombe, N. M., Swindells, M. B., and Thornton, J. M. (1996) Protein clefts in molecular recognition and function. *Protein Sci.* 5, 2438.
- (19) Lane, T. W., and Morel, F. M. M. (2000) A biological function for cadmium in marine diatoms. *Proc. Natl. Acad. Sci. U. S. A.* 97, 4627–4631.
- (20) Xu, Y., Feng, L., Jeffrey, P. D., Shi, Y., and Morel, F. M. M. (2008) Structure and metal exchange in the cadmium carbonic anhydrase of marine diatoms. *Nature* 452, 56–61.
- (21) Lane, T. W., Saito, M. A., George, G. N., Pickering, I. J., Prince, R. C., and Morel, F. M. M. (2005) Biochemistry A cadmium enzyme from a marine diatom. *Nature* 435, 42–42.
- (22) Chan, J., Huang, Z., Watt, I., Kille, P., and Stillman, M. J. (2007) Characterization of the conformational changes in recombinant human metallothioneins using ESI-MS and molecular modeling. *Can. J. Chem.* 85, 898–912.
- (23) Coleman, J. E. (1967) Mechanism of action of carbonic anhydrase: Substrate, sulfonamide, and anion binding. *J. Biol. Chem.* 242, 5212–5219.
- (24) Chen, R. F., and Kernohan, J. C. (1967) Combination of bovine carbonic anhydrase with a fluorescent sulfonamide. *J. Biol. Chem.* 242, 5813–5823.
- (25) Pinter, T. B. J., and Stillman, M. J. (2014) The zinc balance: Competitive zinc metalation of carbonic anhydrase and metallothionein 1A. *Biochemistry* 53, 6276–6285.
- (26) Mason, A. Z., Moeller, R., Thrippleton, K. A., and Lloyd, D. (2007) Use of stable isotopically enriched proteins and directly coupled high-performance liquid chromatography inductively coupled plasma mass spectrometry for quantitatively monitoring the transfer of metals between proteins. *Anal. Biochem.* 369, 87–104.
- (27) Zaia, J., Fabris, D., Wei, D., Karpel, R. L., and Fenselau, C. (1998) Monitoring metal ion flux in reactions of metallothionein and drug-modified metallothionein by electrospray mass spectrometry. *Protein Sci.* 7, 2398–2404.
- (28) Zalewska, M., Trefon, J., and Milnerowicz, H. (2014) The role of metallothionein interactions with other proteins. *Proteomics* 14, 1343–1356.
- (29) Roesijadi, G., Bogumil, R., Vasák, M., and Kägi, J. H. (1998) Modulation of DNA binding of a tramtrack zinc finger peptide by the metallothionein-thionein conjugate pair. *J. Biol. Chem.* 273, 17425–17432.
- (30) Ejnik, J., Muñoz, A., Gan, T., Shaw, C. F., III, and Petering, D. (1999) Interprotein metal ion exchange between cadmium-carbonic anhydrase and apo-or zinc-metallothionein. *J. Biol. Inorg. Chem.* 4, 784–790.
- (31) Kręzel, A., and Maret, W. (2007) Dual nanomolar and picomolar Zn (II) binding properties of metallothionein. *J. Am. Chem. Soc.* 129, 10911–10921.
- (32) Petering, D. H., Zhu, J., Krezoski, S., Meeusen, J., Kiekenbush, C., Krull, S., Specher, T., and Dughish, M. (2006) Apo-metallothionein emerging as a major player in the cellular activities of metallothionein. *Exp. Biol. Med.* 231, 1528–1534.
- (33) Lindskog, S., and Nyman, P. O. (1964) Metal-binding properties of human erythrocyte carbonic anhydrases. *Biochim. Biophys. Acta, Spec. Sect. Enzymol. Subj.* 85, 462–474.
- (34) Kiefer, L. L., Krebs, J. F., Paterno, S. A., and Fierke, C. A. (1993) Engineering a cysteine ligand into the zinc binding site of human carbonic anhydrase II. *Biochemistry* 32, 9896–9900.
- (35) Kidani, Y., and Hirose, J. (1977) Coordination chemical studies on metalloenzymes II. Kinetic behavior of various types of chelating agents towards bovine carbonic anhydrase. *J. Biochem. (Tokyo)* 81, 1383–1391.
- (36) Coleman, J. E. (1965) Human carbonic anhydrase. Protein conformation and metal ion binding. *Biochemistry* 4, 2644–2655.
- (37) Pinter, T. B., and Stillman, M. J. (2014) The zinc balance: Competitive zinc metalation of carbonic anhydrase and metallothionein 1A. *Biochemistry* 53, 6276–6285.
- (38) Mason, A. Z., Perico, N., Moeller, R., Thrippleton, K., Potter, T., and Lloyd, D. (2004) Metal donation and apo-metalloenzyme activation by stable isotopically labeled metallothionein. *Mar. Environ. Res.* 58, 371–375.
- (39) Irvine, G. W., Duncan, K. E., Gullons, M., and Stillman, M. J. (2015) Metalation kinetics of the human α -metallothionein 1a fragment is dependent on the fluxional structure of the apo-protein. *Chem. - Eur. J.* 21, 1269–1279.
- (40) Li, T.-Y., Kraker, A. J., Shaw, C. F., and Petering, D. H. (1980) Ligand substitution reactions of metallothioneins with EDTA and apo-carbonic anhydrase. *Proc. Natl. Acad. Sci. U. S. A.* 77, 6334–6338.
- (41) Eriksson, A. E., Jones, T. A., and Liljas, A. (1988) Refined structure of human carbonic anhydrase II at 2.0 Å resolution. *Proteins: Struct., Funct., Genet.* 4, 274–282.